

Scaling property of flux fluctuations from random walks

Sooyeon Yoon, Soon-Hyung Yook, and Yup Kim*

Department of Physics and Research Institute for Basic Sciences, Kyung Hee University, Seoul 130-701, Korea

(Received 16 July 2007; published 7 November 2007)

We study dynamical scaling of flux fluctuation $\bar{\sigma}(t)$ from the one-random-walker model on regular lattices and complex networks and compare it to the surface width $W(t)$ of a corresponding growth model. On the regular lattices, we analytically show that $\bar{\sigma}(t)$ undergoes a crossover from the nontrivial scaling regime to the trivial one by increasing time t , and we verify the results by numerical simulations. In contrast to the results on the regular lattices, $\bar{\sigma}(t)$ does not show any crossover behavior on complex networks and satisfies the scaling relation $\bar{\sigma}(t) \sim t^{1/2}$ for any t . On the other hand, we show that $W(t)$ of the corresponding model on complex networks has two different scaling regimes, $W \sim t^{1/2}$ for $t \ll N$ and $W(t) \sim t$ for $t \gg N$.

DOI: 10.1103/PhysRevE.76.056104

PACS number(s): 89.75.Da, 05.40.-a

I. INTRODUCTION

Various topological and dynamical properties of networks arising from real systems have attracted many researchers in diverse fields [1–4]. The inherent complexity of networks causes rich behaviors in the dynamical properties of the physical systems depending on the structure of the underlying networks [1–4]. The random walk is one such example. The random walk has been widely investigated to understand the elementary dynamical processes of physical systems on networks [5–13] and also has many practical applications to real world systems such as information searching and routing strategy in the Internet [14–18]. Especially flux to the networks and its fluctuation should be very important to physically understand dynamic flows in the networks. According to the previous studies [19,20], the flux fluctuation σ_i of a node i shows the power-law dependence on the mean flux $\langle f_i \rangle$ as

$$\sigma_i \sim \langle f_i \rangle^\alpha. \quad (1)$$

Moreover, the theory suggested that there exist two distinct universality classes of systems. The first class consists of the $\alpha=1/2$ systems. When the internal intrinsic dynamics mainly control the system, the system belongs to the $\alpha=1/2$ class. Packets transportation in the Internet routers [21] and information carried by electric currents in a microprocessor [22] are members of this class. The second class is the $\alpha=1$ class. If the dispersion of input flux to the networks is the dominant dynamical process, the system belongs to the $\alpha=1$ class. The fluctuation on the world-wide-web (WWW) [23], the traffic at different locations in the highway system, and the stream flow of river network belong to the $\alpha=1$ class [19].

To understand the origin of two distinct classes, flux fluctuation of a multi-random-walker model on a complex network was investigated [19]. In the model, N_{rw} walkers are initially distributed to randomly chosen nodes of the underlying network in each experiment $d(d=1, 2, \dots, D)$. After each random walker takes the preassigned t steps, the total number f_{id} of visitations of node i is measured. If N_{rw} varies

in each experiment, f_{id} are affected not only by the intrinsic properties of the random walks but also by variations of N_{rw} . From the data set $\{f_{id}\}$, one can calculate the mean flux of a site i ,

$$\langle f_i(t) \rangle = \frac{1}{D} \sum_{d=1}^D f_{id}(t), \quad (2)$$

and the fluctuation $\sigma_i^2(t)$,

$$\sigma_i^2(t) = \langle f_i^2(t) \rangle - \langle f_i(t) \rangle^2. \quad (3)$$

On the scale-free networks (SFNs) with the degree exponent $\gamma=3$, it was found that $\sigma_i(t)$ depends on $\langle f_i(t) \rangle$ as Eq. (1) with two possible exponents, $\alpha=1/2$ and $\alpha=1$ [19]. The results of the multi-random-walker model supported that the real systems such as Internet routers, WWW, and so on can be classified into two distinct universality classes by the competition between the intrinsic internal dynamics and the external input variations. In contrast to the results of Refs. [19,20], another study [24] made efforts to find the system which has nontrivial α , i.e., $\alpha \neq 1/2$ or 1 by introducing impacts depends on the degree of a node. In this paper, we will show that the flux fluctuation of one random walker on regular lattices (homogeneous networks) naturally has nontrivial exponent α by studying the average flux fluctuation.

The average flux fluctuation $\bar{\sigma}$ over nodes on the network with N nodes is defined as

$$\bar{\sigma}^2(t) \equiv \frac{1}{N} \sum_{i=1}^N \sigma_i^2(t) = \frac{1}{N} \sum_{i=1}^N \left[\frac{1}{D} \sum_{d=1}^D f_{id}^2(t) - \left(\frac{1}{D} \sum_{d=1}^D f_{id}(t) \right)^2 \right]. \quad (4)$$

The mean flux $\langle f_i(t) \rangle$ should be proportional to t as $\langle f_i(t) \rangle = c_i t$, where c_i is a constant dependent on the structure of the given underlying topology. From Eqs. (1) and (4), one can obtain

$$\bar{\sigma}(t) = C t^\alpha, \quad (5)$$

where $C^2 \equiv \frac{1}{N} \sum_{i=1}^N c_i^2$. Based on Eq. (5), we can also easily understand the power-law behavior (1) by analyzing the dependence of $\bar{\sigma}$ on t for more broad range of t .

*ykim@khu.ac.kr

In this paper, we study the dynamical scaling properties of $\bar{\sigma}(t)$ using a one-random-walker (RW) model ($N_{\text{rw}}=1$) on several networks.

Since no variation of external flux exists or $\Delta N_{\text{rw}}=0$, the dynamics of the system is governed only by the internal intrinsic dynamics of RW. On regular lattices, especially on one- and two-dimensional ($1, 2d_s$) lattices, we find the nontrivial exponent $\alpha \neq 1/2, 1$ in the infinite system ($L^{d_s} \rightarrow \infty$). The nontrivial α is physically related to the recurrence of the random walk [25–27]. The flux of a site i depends on the conditional probability that RW visits the site at a time t under the condition that the walker has visited the same site at an earlier time $t' (< t)$. However, in finite-sized 1 and $2d_s$ lattices, there exists a crossover behavior from the nontrivial regime ($\alpha \neq 1/2, 1$) to the trivial regime ($\alpha = 1/2$) in the limit $t \rightarrow \infty$. This comes from the fact that the visitation probability of each site becomes constant in the limit $t \rightarrow \infty$ for the finite-sized lattices and thus the dynamics becomes similar to that of the random deposition [28]. In contrast, the scaling relation (5) with trivial exponent $\alpha = 1/2$ holds for any time t in regular lattices with $d_s \geq 3$. The trajectory of RW on lattices with $d_s \geq 3$ is transient in early time t , therefore $\bar{\sigma}(t)$ follows Eq. (5) with $\alpha = 1/2$. In the long-time limit, the random deposition occurs by the finite size effect, the dynamical behavior of $\bar{\sigma}(t)$ does not show the crossover behavior.

The dynamical behavior of $\bar{\sigma}(t)$ in complex networks also follows Eq. (5) with $\alpha = 1/2$ without showing any crossover behavior. The scaling behavior seems to be the same as that of $d_s \geq 3$ regular lattices. However, the dynamical origin of the scaling behavior in complex network is different from that in regular lattices. In early time, the dynamics of RW becomes the same as that of random deposition, because RW is transient and cannot see the whole structure of the system. Therefore, the $\langle f_i(t) \rangle$ of each node linearly grows with time and the $\bar{\sigma}(t)$ increases as Eq. (5) with $\alpha = 1/2$. However, in the long-time limit, the dynamics of RW is affected by the heterogeneity of complex network. Since the probability P_i that a RW visits a node i is proportional to the number of degree k_i [10] as $P_i(t \rightarrow \infty) = k_i / \sum_j k_j$, the mean flux of each node increases depending on its degree k in the long-time limit. Thus we should analyze the dependence of averaged flux fluctuation on degree, $\bar{\sigma}(k)$, to fully understand the flux dynamics.

$\bar{\sigma}(t)$ is physically related to the surface width $W(t)$ of a corresponding growth model, because the flux configuration $\{f_{id}\}$ can be mapped into the height configuration $\{h_{id}\}$ in the growth model. In the growth model, RW drops a particle whenever it visits a site i and thus $f_{id}(t) = h_{id}(t)$. Therefore, the fluctuation of $h_{id}(t)$, defined by the surface width W [28], is somehow physically related to $\bar{\sigma}(t)$. The surface width in the model is

$$W^2(t) = \frac{1}{D} \sum_{d=1}^D \left[\frac{1}{N} \sum_{i=1}^N h_{id}^2(t) - \left(\frac{1}{N} \sum_{i=1}^N h_{id}(t) \right)^2 \right]. \quad (6)$$

In normal lattice systems, the difference between $W(t)$ and $\bar{\sigma}(t)$ becomes negligible, since there are no breakdowns of spatial or temporal symmetry such as the local columnar

defect [28] or temporally colored noise [28]. On the other hand, the intrinsic difference exists between $\bar{\sigma}(t)$ and $W(t)$ on complex network, since $\langle f_i \rangle$ depends on the degree k for large t . In this sense it is physically important to compare $W(t)$ and $\bar{\sigma}(t)$ on complex network to understand the intrinsic properties of RW on the network.

In this paper, we will focus on the scaling property of the globally averaged flux fluctuation of one random walker on regular lattices and complex networks. The scaling property on regular lattices will be studied by using continuum equation with colored noise originated from the intrinsic property of RW. We will also study the scaling property by numerical simulations.

II. MODEL

In each experiment or trial d , a RW is initially placed at a randomly chosen site (or node) on a given network. The network has assumed to have N nodes. If the network is a regular lattice, then $N = L^{d_s}$ where L is the lateral size of the lattice. At each time step the walker moves to a randomly chosen node (site) among the nodes (sites) directly linked to the node (site) where the walker is. In each experiment d , we measure the dependence of the number of visits $f_{id}(t)$ on the time step t . By repeating the procedure D times, we calculate $\langle f_{id}(t) \rangle$, $\sigma_i^2(t)$, and $\bar{\sigma}(t)$ from Eqs. (2)–(4).

III. CONTINUUM EQUATION APPROACH

Let us consider a continuum version of random walks to understand the scaling property of $\bar{\sigma}(t)$. To calculate the incoming flux to the site \vec{r} at time t , we introduce the stochastic variable $\eta(\vec{r}, t)$. If the RW visits \vec{r} at time t , $\eta(\vec{r}, t) = 1$, otherwise, $\eta(\vec{r}, t) = 0$. In the limit $L \rightarrow \infty$ RW will satisfy the diffusion equation and then

$$\begin{aligned} \langle \eta(\vec{r}, t) \rangle &= \frac{1}{(2\pi t)^{d_s/2}} \exp\left(-\frac{(\vec{r} - \vec{r}_0)^2}{2t}\right), \\ \langle \eta(\vec{r}, t) \eta(\vec{r}', t') \rangle &= \frac{1}{(2\pi t)^{d_s/2}} \exp\left(-\frac{(\vec{r} - \vec{r}_0)^2}{2t}\right) \frac{1}{(2\pi |t - t'|)^{d_s/2}} \\ &\quad \times \exp\left(-\frac{(\vec{r} - \vec{r}')^2}{2|t - t'|}\right), \end{aligned} \quad (7)$$

where \vec{r}_0 is the initial position of RW. Physically $\langle \eta(\vec{r}, t) \rangle$ means the probability to find the RW at site \vec{r} at time t and $\langle \eta(\vec{r}, t) \eta(\vec{r}', t') \rangle$ is the joint probability that the RW is at site \vec{r} at time t and at site \vec{r}' at time t' . The evolution of the $f(\vec{r}, t)$ in time is given by the continuum equation,

$$\frac{df(\vec{r}, t)}{dt} = \eta(\vec{r}, t). \quad (8)$$

The solution of Eq. (8) is $f(\vec{r}, t) = \int_0^t \eta(\vec{r}, t') dt'$. From Eqs. (7) and (8), we obtain the expression of $\bar{\sigma}(t)$. When $t' < t$, the average of $f^2(\vec{r}, t)$ over the sites (spaces), $\overline{f^2(\vec{r}, t)}$, becomes

$$\begin{aligned} \overline{f^2(\vec{r}, t)} &= \frac{1}{L^{d_s}} \int d\vec{r} f^2(\vec{r}, t) \\ &\approx \frac{1}{L^{d_s}} \int d\vec{r} \int_0^t \int_0^{t'} \langle \eta(\vec{r}, t') \eta(\vec{r}, t'') \rangle dt' dt''. \end{aligned} \quad (9)$$

By averaging over initial position \vec{r}_0 ,

$$\overline{f^2(\vec{r}, t)} \approx \frac{1}{(2\pi)^{d_s/2}} \frac{1}{L^{d_s}} \int_0^t \int_0^{t'-1} |t' - t''|^{-d_s/2} dt' dt''. \quad (10)$$

Similarly,

$$\overline{f(\vec{r}, t)^2} \approx \frac{t^2}{L^{2d_s}}. \quad (11)$$

From Eqs. (10) and (11), $\bar{\sigma}(t)$ becomes

$$\bar{\sigma}^2(t) = \overline{f(\vec{r}, t)^2} - \overline{f(\vec{r}, t)}^2 \approx \begin{cases} \frac{t^{2d_s}}{L} - \frac{t^2}{L^2} & \text{for } d_s = 1, \\ \frac{(t \ln t)^{1/2}}{L^2} - \frac{t^2}{L^4} & \text{for } d_s = 2, \\ \frac{t}{L^{d_s}} - \frac{t^2}{L^{2d_s}} & \text{for } d_s \geq 3. \end{cases} \quad (12)$$

When $t \ll L^2$ ($L \rightarrow \infty$), the dominant time dependence of $\sigma(t)$ becomes

$$\bar{\sigma}(t) \approx \begin{cases} \frac{t^{3/4}}{L^{1/2}} & \text{for } d_s = 1, \\ \frac{(t \ln t)^{1/2}}{L} & \text{for } d_s = 2, \\ \frac{t^{1/2}}{L^{d_s/2}} & \text{for } d_s \geq 3. \end{cases} \quad (13)$$

However, when $t \gg L^2$, the probability $\langle \eta(\vec{r}, t) \rangle$ becomes the same as $\langle \eta(\vec{r}, t) \rangle = 1/L^{d_s}$ for any \vec{r} . Thus the $\bar{\sigma}(t)$ shows similar dynamical property to that of the random deposition as

$$\bar{\sigma}(t \gg L^{d_s}) \sim t^{1/2} \quad (14)$$

in regular lattices and we obtain a trivial exponent $\alpha = 1/2$ for $t \gg L^2$.

IV. SIMULATION RESULTS

Now we show the results of numerical simulation to confirm the scaling relations derived in the preceding section. In the measurement of $\bar{\sigma}(t)$, we use lattices of $L = 2^6, \dots, 2^{10}$ for $1d_s$, $L = 2^7, \dots, 2^{10}$ for $2d_s$, and $L = 2^7$ for $3d_s$. The number of experiments is $D = 100$ and the walker takes $t = 2 \times 10^8$ steps for $1d_s$, $t = 10^8$ steps for $2d_s$, and $t = 10^7$ steps for $3d_s$ in each experiment.

The data in Fig. 1(a) show a crossover from the nontrivial regime [Eq. (13)] to the trivial one [Eq. (14)] in $1d_s$. From the best fit of Eq. (5) to the data in Fig. 1(a), we obtain $\alpha = 0.75(1)$ for $10^1 \leq t \leq 10^5$ and $\alpha = 0.50(1)$ for $10^6 \leq t \leq 2 \times 10^8$. This result agrees very well with our analytic expectation that $\alpha = 3/4$ for $t \ll L^2$ and $\alpha = 1/2$ when $t \gg L^2$ in $1d_s$. In the inset of Fig. 1(a) we show that the dynamical scaling

$$\bar{\sigma}(t) = t^{1/2} f(t/L^2) \quad (15)$$

holds very well in $1d_s$. From Eqs. (13) and (14) the scaling function $f(x)$ should satisfy $f(\infty) = \text{const}$ and $f(x) = x^{1/4}$ for x

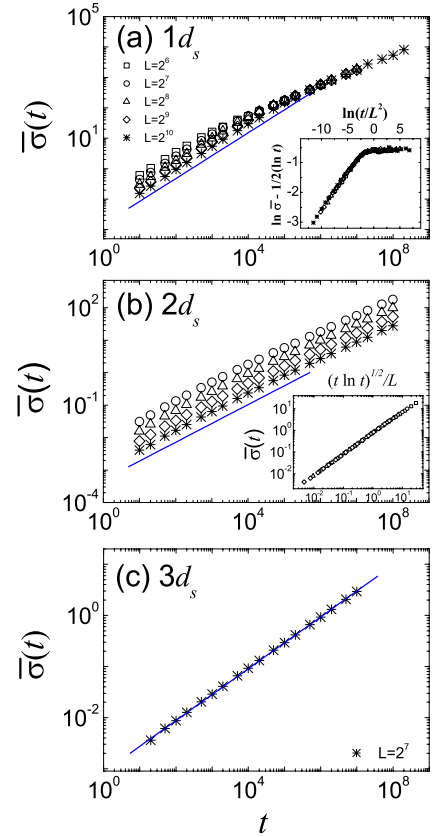


FIG. 1. (Color online) Plots of $\bar{\sigma}(t)$ of the one-random-walker model on (a) one-, (b) two-, and (c) three-dimensional regular lattices. Solid lines are simple fits to the relation (5) to get $\alpha = 0.75(1) \approx 3/4$ for $1d_s$ (a), $\alpha = 0.58(1)$ for $2d_s$ (b), and $\alpha = 0.50(1) \approx 1/2$ for $3d_s$ (c). The inset of (a) shows that the dynamical scaling $\bar{\sigma}(t) = t^{1/2} f(t/L^2)$ holds well in $1d_s$. The inset of (b) shows the existence of the logarithmic correction as $\bar{\sigma}(t) \approx (t \ln t)^{1/2} / L$ in the early time ($t \ll L^2$) in $2d_s$.

$\ll 0$, which are also confirmed numerically in the inset of Fig. 1(a).

In $2d_s$, we obtain $\alpha = 0.58(1)$ for $t < 10^6$ and $\alpha = 0.51(1)$ for $t > 10^6$ by the simple linear fit of Eq. (5) to the data in Fig. 1(b). However, Eq. (13) predicts the existence of a logarithmic correction for $t \ll L^2$. In order to check the existence of such correction, we plot $\bar{\sigma}(t)$ against $(t \ln t)^{1/2} / L$ in the inset of Fig. 1(b) by using the data for $t \leq 10^6$. As shown in the inset the relation $\bar{\sigma}(t) \approx (t \ln t)^{1/2} / L$ holds very well in $2d_s$ regardless of the lateral size L .

In $3d_s$, $\bar{\sigma}(t)$ does not show any crossover behavior. [See Fig. 1(c).] From the data in Fig. 1(c) one can see $\bar{\sigma}(t) \approx t^\alpha$ with $\alpha = 0.51(1)$ holds for any time t .

These results in Fig. 1 agree very well with our analytic expectation in Sec. III for the crossover behavior of $\bar{\sigma}(t)$ from the nontrivial regime to the trivial one in regular lattices. We also check that in the regular lattices the surface width $W(t)$ shows exactly the same dynamical behavior as $\bar{\sigma}(t)$.

Since the dynamical properties of many physical systems are known to be affected by the heterogeneity of the underlying structure [17,29], we also investigate the effect of the

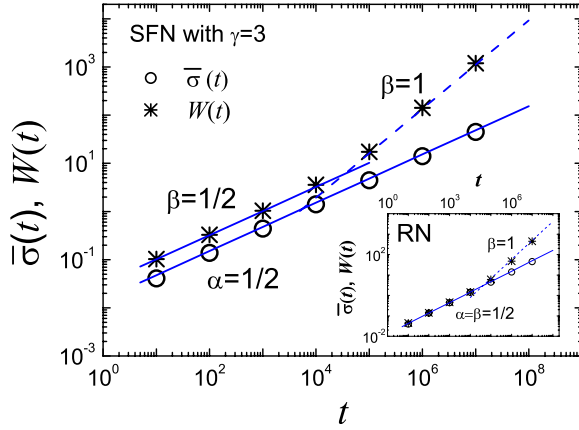


FIG. 2. (Color online) Plots of $\bar{\sigma}(t)$ and $W(t)$ on scale-free network (SFN, main figure) and random network (RN, inset). The number of nodes are $N=10^4$ and the degree exponent of the SFN is $\gamma=3$. The solid lines represent the power law $\bar{\sigma}(t) \sim t^\alpha$ and $W \sim t^\beta$ with $\alpha=\beta=1/2$ and the dashed lines correspond to the power law $W(t) \sim t^\beta$ with $\beta=1$. The value of α is not changed. In contrast, the value of β is changed from $1/2$ to 1 when $t \gg N$ for the SFN and RN.

underlying topology on the flux fluctuation of our model. For this, we also consider two types of complex networks of size $N=10^4$; random networks (RNs) and scale-free networks [1–4]. As shown in Fig. 2, the scaling relation of $\bar{\sigma}(t)$ satisfies $\bar{\sigma}(t) \sim t^\alpha$ for any t with the exponent $\alpha \approx 1/2$ on both RNs [$\alpha=0.51(1)$] and SFNs [$\alpha=0.50(1)$]. The dynamical property of $\bar{\sigma}(t)$ can be explained by the random ballistic deposition in early time regime when there is no variation of the external flux regardless of the heterogeneity of underlying structures. This implies that the random walker cannot explore the entire network, and the heterogeneity does not affect the order of average over space and experiment in Eqs. (4) and (6). Thus, both $\bar{\sigma}(t)$ and $W(t)$ are expected to show the same scaling behavior as $\bar{\sigma}(t) \sim t^{1/2}$ and $W(t) \sim t^{1/2}$ in the early time regime.

However, if t is sufficiently large (or $t \rightarrow \infty$), the probability to find a walker at each node becomes uneven. Therefore, the topological heterogeneity can cause a difference between $\bar{\sigma}(t)$ and $W(t)$ as shown in Fig. 2. This difference can be analytically understood. In the limit $t \rightarrow \infty$, $\langle f_i(t) \rangle \approx k_i t$ [10]. So we obtain for $t \gg L$,

$$\begin{aligned} W^2 &= \frac{1}{N} \sum_i \frac{k_i^2}{(\sum_j k_j)^2} t^2 - \left(\frac{1}{N} \sum_i \frac{k_i}{\sum_j k_j} t \right)^2 \\ &= \frac{A}{N} \left[\sum_i k_i^2 - \frac{1}{N} \left(\sum_i k_i \right)^2 \right] t^2 \sim t^{2\beta} \quad (\beta=1), \end{aligned} \quad (16)$$

where $A=(1/\sum_j k_j)^2$. From the data in Fig. 2 we obtain $\beta=0.92(1)$ on SFN and $\beta=0.93(3)$ on RN when $t \gg N$.

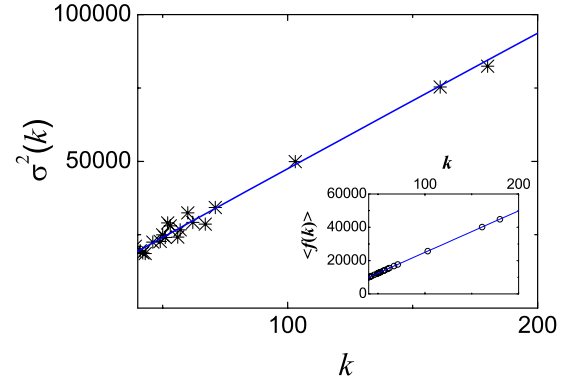


FIG. 3. (Color online) Plots of $\sigma^2(k)$ and $\langle f(k) \rangle$ (inset) against k on SFN with $\gamma=3$. The data is taken on the network size $N=10^4$ at time $t=10^7$. The solid lines represent $\sigma^2(k) \sim k$ and $\langle f(k) \rangle \sim k$.

In contrast to $W(t)$, $\bar{\sigma}(t)$ still follows the scaling relation $\bar{\sigma}(t) \sim t^{1/2}$ for $t \gg N$ on complex networks (see Fig. 2). The average incoming flux of node i of degree k_i increases as $\langle f_i(t) \rangle \sim k_i t$ [10]. Then, from Eq. (1) σ_i becomes

$$\sigma_i \sim \langle f_i \rangle^\alpha \sim k_i^\alpha. \quad (17)$$

We measure $\sigma^2(k)$ and $\langle f(k) \rangle$ on SFN with $N=10^4$ and $t=10^7$ to find $\langle f(k) \rangle \sim k$ and $\sigma^2(k) \sim k$ for reasonably large k as shown in Fig. 3. Therefore, we expect $\sigma^2(k) \sim k \sim \langle f(k) \rangle$ and $\alpha=1/2$ from Eq. (1).

V. CONCLUSION

We study the scaling properties of the flux fluctuation of one-RW model on various underlying structures and compare the results with the surface width of the corresponding growth model. We analytically derive the scaling relation of $\bar{\sigma}(t)$ on the regular lattices of various dimensions. We find that $\bar{\sigma}(t)$ scales in a nontrivial way when $t \ll L^2$ in 1 and $2d_s$. For $t \gg L^2$, $\bar{\sigma}(t)$ scales as $\bar{\sigma}(t) \sim t^{1/2}$ in all dimensions due to the finiteness of the lattices. In order to study the effect of the heterogeneity of the underlying topology on the scaling properties of $\bar{\sigma}(t)$, we also investigate the dynamic property of one RW model on RNs and SFNs. We show that $W \sim t^{1/2}$ for $t \ll N$ and $W(t) \sim t$ when $t \gg N$ due to the heterogeneity of the underlying topology. In contrast to $W(t)$, we find that $\bar{\sigma}(t)$ scales as $\bar{\sigma}(t) \sim t^{1/2}$ for all t . These results are also verified by numerical simulations.

ACKNOWLEDGMENTS

The authors thank Professor J. D. Noh for helpful suggestions and critical comments. This work was supported by the Korea Science and Engineering Foundation (KOSEF) grant funded by the Korea government (MOST) (Grants Nos. R01-2007-000-10910-0, R01-2006-000-10470-0, and F01-2006-000-10093-0).

- [1] D. J. Watts and S. H. Strogatz, *Nature (London)* **393**, 440 (1998).
- [2] A.-L. Barabási and R. Albert, *Science* **286**, 509 (1999); R. Albert and A.-L. Barabási, *Rev. Mod. Phys.* **74**, 47 (2002).
- [3] M. E. J. Newman, S. H. Strogatz, and D. J. Watts, *Phys. Rev. E* **64**, 026118 (2001).
- [4] S. N. Dorogovtsev and J. F. F. Mendes, *Adv. Phys.* **51**, 1079 (2002).
- [5] S. Jespersen, I. M. Sokolov, and A. Blumen, *Phys. Rev. E* **62**, 4405 (2000).
- [6] B. Tadić, *Eur. Phys. J. B* **23**, 221 (2001).
- [7] J. Lahtinen, J. Kertész, and K. Kaski, *Phys. Rev. E* **64**, 057105 (2001).
- [8] E. Almaas, R. V. Kulkarni, and D. Stroud, *Phys. Rev. E* **68**, 056105 (2003).
- [9] L. K. Gallos, *Phys. Rev. E* **70**, 046116 (2004).
- [10] J. D. Noh and H. Rieger, *Phys. Rev. Lett.* **92**, 118701 (2004).
- [11] S. Yoon, S. Lee, S.-H. Yook, and Yup Kim, *Phys. Rev. E* **75**, 046114 (2007).
- [12] L. F. Costa and G. Travieso, *Phys. Rev. E* **75**, 016102 (2007).
- [13] S. Lee, S.-H. Yook, and Yup Kim, e-print arXiv:cond-mat/0701070.
- [14] F. Jasch and A. Blumen, *Phys. Rev. E* **63**, 041108 (2001).
- [15] L. A. Adamic, R. M. Lukose, A. R. Puniyani, and B. A. Huberman, *Phys. Rev. E* **64**, 046135 (2001).
- [16] R. Guimerá, A. Díaz-Guilera, F. Vega-Redondo, A. Cabrales, and A. Arenas, *Phys. Rev. Lett.* **89**, 248701 (2002).
- [17] S. Lee, S.-H. Yook, and Yup Kim, *Phys. Rev. E* **74**, 046118 (2006).
- [18] S. Lee, S.-H. Yook, and Yup Kim, *Physica A* **385**, 743 (2007).
- [19] M. A. de Menezes and A.-L. Barabási, *Phys. Rev. Lett.* **92**, 028701 (2004).
- [20] M. A. de Menezes and A.-L. Barabási, *Phys. Rev. Lett.* **93**, 068701 (2004).
- [21] A. Vazquez, R. Pastor-Satorras, and A. Vespignani, *Phys. Rev. E* **65**, 066130 (2002).
- [22] R. F. Cancho, C. Janssen, and R. V. Sole, *Phys. Rev. E* **64**, 046119 (2001).
- [23] S. Lawrence and L. Giles, *Science* **280**, 98 (1998).
- [24] Z. Eisler and J. Kertész, *Phys. Rev. E* **71**, 057104 (2005).
- [25] S. Redner, *A Guide to First-Passage Processes* (Cambridge University Press, Cambridge, 2001).
- [26] G. H. Weiss and R. J. Rubin, *Adv. Chem. Phys.* **52**, 363 (1983); G. H. Weiss, *Aspects and Applications of the Random Walk* (North-Holland, Amsterdam, 1994).
- [27] B. D. Hughes, *Random Walks and Random Environments* (Oxford University Press, Oxford, 1995).
- [28] *Dynamics of Fractal Surfaces*, edited by F. Family and T. Vicsek (World Scientific, Singapore, 1991); A.-L. Barabási and H. E. Stanley, *Fractal Concepts in Surface Growth* (Cambridge University Press, Cambridge, 1995); J. Krug, *Adv. Phys.* **46**, 139 (1997); T. Halpin-Healy and Y.-C. Zhang, *Phys. Rep.* **254**, 215 (1995); E. Medina, T. Hwa, M. Kardar, and Y.-C. Zhang, *Phys. Rev. A* **39**, 3053 (1989).
- [29] S.-H. Yook and M. A. de Menezes, *Europhys. Lett.* **72**, 541 (2005).